MEDDOCS Open Access Publisher

ISSN: 2637-4927

Annals of Biotechnology

Open Access | Research Article

Unlocking the Genetic Potential of Florida's Economically Important, Vulnerable, and Critically Imperiled Native Palms: A Transcriptomic Landscape Analysis

Madhugiri Nageswara-Rao[1*#]; Prasad Gandahm[2#]; Vaishali M Gopala[1#]; Daniel A Tucker[3,4]; Amir A Khoddamzadeh[3]; Niranjan Baisakh[2]

[1]Subtropical Horticultural Research Station, USDA-ARS, Coral Gables, FL, USA.

[2]School of Plant, Environmental and Soil Sciences, Louisiana State University Agricultural Center, Baton Rouge, LA, USA.

[3]Florida International University, Institute of the Environment, Earth and Environment Department, Miami, FL, 33199, USA.

[4]Montgomery Botanical Center, Coral Gables, FL 33156, USA.

[#]These authors contributed equally to this article.

***Corresponding Author(s): Madhugiri Nageswara-Rao**

Subtropical Horticultural Research Station, USDA-ARS, Coral Gables, FL, USA.

Tel: 786-573-7050; Email: mnrbhav@gmail.com; Madhugiri.Nageswara-Rao@usda.gov

Received: June 04, 2026

Accepted: June 22, 2026

Published Online: June 29, 2026

Journal: Annals of Biotechnology

Publisher: MedDocs Publishers LLC

Online edition: http://meddocsonline.org/

Copyright: © Nageswara-Rao M (2026). *This Article is distributed under the terms of Creative Commons Attribution 4.0 International License*

Keywords: Comparative gene expression; Germplasm characterization; Molecular mechanisms and markers; Native species; Ornamentals; Transcriptomes.

Abstract

Native palm species are important components of Florida's coastal ecosystems and ornamental horticulture, yet genomic resources for these taxa remain limited. In this study, we performed a comparative transcriptomic analysis of three native Florida palms, *Pseudophoenix sargentii*, *Sabal miamiensis*, and *Sabal palmetto*, to generate foundational molecular resources and examine transcriptional divergence among species. RNA sequencing of leaf tissues produced over 654 million raw reads of which approximately 577 million high-quality reads were retained after filtering. *De novo* assembly yielded 455,094 contigs that were further filtered to 82,949 transcripts representing 42,834 non-redundant unigenes. Differential expression analysis revealed substantial transcriptional divergence among species, with 6,038 Differentially Expressed Unigenes (DEUs) identified between the two *Sabal* species and more than 27,000 genes distinguishing each *Sabal* species from *P. sargentii*. Functional annotation and gene ontology enrichment analyses indicated that many DEUs were associated with metabolic processes, transcriptional regulation, and stress-response pathways. Transcriptome mining also identified 10,145 Simple Sequence Repeats (SSRs) and 23,876 Single Nucleotide Polymorphisms (SNPs) within expressed gene regions, providing valuable molecular markers for future genetic studies. Collectively, this study provides the first comprehensive comparative transcriptomic resource for these native Florida palms and establishes a foundation for future research on palm biology, conservation genetics, and the development of molecular markers to support germplasm characterization and marker-assisted breeding in ornamental palms.

Cite this article: Nageswara-Rao M, Gandahm P, Gopala VM, Tucker DA, Khoddamzadeh AA, et al. Unlocking the Genetic Potential of Florida's Economically Important, Vulnerable, and Critically Imperiled Native Palms: A Transcriptomic Landscape Analysis. Ann Biotechnol. 2026; 9(1): 1033.

Introduction

Florida is one of the leading producers of ornamental plants in the United States, with its floriculture and landscape horticulture industries contributing substantially to the state's economy. These sectors generated $21.08 billion in total output, supported 232,648 jobs, and contributed $13.17 billion in value-added benefits [1]. Sustaining this growth depends heavily on the continuous development and availability of new, locally adapted germplasm to meet evolving consumer preferences. Among ornamental plants, palms, woody ornamentals, and flowering species have collectively driven a 13% increase in wholesale value since 2018, with palms emerging as particularly iconic elements of tropical and subtropical landscapes in Florida and globally [2-4].

Beyond their aesthetic appeal, palms play a central role in shaping urban and natural landscapes. Once used primarily as accent plants, they are now integral components of urban forests, contributing to cultural identity, ecological stability, and tourism economies in tropical regions [4-6]. Their commercial success is further supported by practical advantages over broadleaf trees, including efficient space utilization due to their columnar growth habit, reduced maintenance requirements, and resilience during transplantation. These attributes make palms highly desirable for landscaping applications ranging from urban infrastructure to commercial developments [6-10]. In addition, palms hold deep cultural significance across tropical and subtropical regions, symbolizing peace, fertility, and prosperity [11]. Southern Florida, particularly Miami-Dade County, serves as the epicenter of this industry, accounting for over $7.5 billion in sales and hosting approximately 2,400 registered nurseries specializing in tropical ornamentals (https://sfyl.ifas.ufl.edu/miami-dade/agriculture/ornamental-production/).

However, the rapid expansion of the ornamental plant trade has raised concerns regarding biodiversity loss, invasive species introduction, and climate vulnerability. Florida is especially susceptible, with nearly 1,400 non-native plant species now established in the state [12-15]. In contrast, only twelve palm species are native to Florida, yet these species play critical ecological roles and hold significant economic value [11,16,17]. For example, *Sabal palmetto*, the state tree of Florida and South Carolina, is highly resilient to extreme weather conditions, including hurricanes, and remains widely cultivated [18]. *Pseudophoenix sargentii* contributes to coastal stabilization and wildlife habitat, while the critically endangered *Sabal miamiensis*, endemic only to the Atlantic Coastal Ridge of southeastern Florida, occurs on alkaline substrates in pine rocklands and scrub [19]. These native palms are increasingly valued for their exceptional tolerance to environmental stresses such as salinity, drought, flooding, fire, and temperature extremes [10,11,17,20].

Despite their importance, native palm populations are under increasing pressure due to overharvesting and habitat loss. Several species now require harvesting permits, including *P. sargentii*, *Roystonea regia*, and *Thrinax radiata*, while *S. miamiensis* was believed to be extinct the wild before being rediscovered recently [21,22]. These challenges highlight a critical gap in conservation and breeding efforts, compounded by the lack of molecular and genomic resources for native palms. In contrast to well-studied species such as date palm (*Phoenix dactylifera*), oil palm (*Elaeis guineensis*), and coconut (*Cocos nucifera*), native Florida palms remain largely uncharacterized at the genetic level [7,8,23]. Currently, no chromosome-scale genome assemblies exist for these species, and transcriptomic data remain limited, restricting efforts to understand stress tolerance and adaptive traits [7,8,23].

In the absence of reference genomes, *de novo* RNA sequencing provides a powerful approach for generating comprehensive transcriptomic resources in non-model species [24]. Tools such as Trinity enable the reconstruction of full-length transcripts and facilitate downstream analyses, including gene expression profiling and functional annotation [25,26,27]. In this study, we present the first *de novo* transcriptome assemblies for three ecologically and economically important native Florida palm species, *P. sargentii*, *S. miamiensis*, and *S. palmetto*, based on leaf RNA-seq data. Our objectives were to establish foundational transcriptomic resources and identify differentially expressed genes and biological pathways underlying species-specific adaptations. This research will support conservation of endangered palm species, improve selection of resilient native palms, sustainable plant breeding, and strengthen ornamental nursery and landscaping industries for the future.

Materials and methods

Plant materials and tissue sampling

Individuals of *P. sargentii*, *S. miamiensis*, and *S. palmetto* were cultivated at the USDA-ARS Subtropical Horticultural Research Station in Miami, Florida (25.6421°N, 80.2944°W). To ensure consistency and tissue health, leaf tissue was collected from the youngest fully expanded frond adjacent to the spear leaf of mature palms, avoiding specimens showing signs of mechanical damage or pathogen infestation. Approximately 50 mg of young green leaf tissue was excised from three different individuals of each of *P. sargentii*, *S. miamiensis*, and *S. palmetto.* The cleaned tissues were immediately flash-frozen in liquid nitrogen to preserve RNA integrity and stored at −80 °C until RNA extraction.

RNA purification, RNA-Seq library preparation, and sequencing

Total RNA was isolated from the young leaf tissue of each species using the Cetyltrimethylammonium Bromide (CTAB) extraction method as described by [28]. The RNA concentration and integrity were assessed by fluorometric quantification with a Qubit system (Thermo Fisher Scientific, Carlsbad, CA) and by examination on a 1% agarose gel. RNA-Seq libraries were constructed for *P. sargentii*, *S. miamiensis*, and *S. palmetto* using 4 µg of total RNA, following the standard protocol supplied with the TruSeq RNA Library Preparation Kit (Illumina Inc., San Diego, CA). The resulting cDNA libraries were quantified using the Qubit Broad Range Assay and quality verified using an Agilent 2100 Bioanalyzer (Agilent Technologies, Santa Clara, CA) with DNA-specific chips. Paired-end sequencing was performed on an Illumina HiSeq high-throughput platform at the University of Illinois Roy J. Carver Biotechnology Center. All sequence reads were submitted to the public NCBI Sequence Read Archive database under BioSample accessions PRJNA1465365.

Sequence data processing

Sequence data were processed following established bioinformatic pipelines [29,30]. Raw sequence reads were evaluated using FastQC v0.12.1 to monitor quality metrics. Low-quality reads and adapter sequences were removed with Trimmomatic v0.39 [31] using the parameter SLIDINGWINDOW:4:15 and reads shorter than 50 bp were discarded. High-quality reads were assembled *de novo* using Trinity v2.15.1 [26]. To mitigate redundancy, sequence clustering was conducted with CD-HIT-

EST [32]. Assembled transcripts were screened against the Rfam database [33] to identify and remove noncoding RNA sequences. Open Reading Frames (ORFs) were predicted using TransDecoder, and only transcripts containing valid ORFs were retained for downstream analyses.

Differential expression of unigenes

Unigene expression levels were quantified using RSEM [34] based on the generated transcriptome reference. Differential expression analysis was performed using DESeq2 [35] with significant thresholds set at $|\log2 \text{ fold change}| \geq 2$, $p \leq 0.05$, and Padj ≤ 0.001. Volcano plots were generated for each species comparison employing the EnhancedVolcano R package, illustrating the distribution of significantly upregulated and downregulated unigenes. Global expression trends across all combinations were visualized as heatmaps using the Pheatmap package in R.

Functional annotation and enrichment of unigenes

Functional characterization of unigenes was achieved through homology-based searches using BLASTn and BLASTx against the NCBI RefSeq plant nucleotide and protein databases and the *Viridiplantae* subset of the Swiss-Prot database with an e-value threshold of 1e−06. Protein domain annotation was conducted using HMMER v3.3.2 (http://hmmer.org) with searches against the Pfam database (https://www.ebi.ac.uk/interpro/download/pfam/). Further functional annotation, including Gene Ontology (GO) classification, was performed using InterProScan (https://www.ebi.ac.uk/interpro/download/interproscan/). GO enrichment analysis utilized Fisher's exact test implemented in the topGO R package and GO terms with $p \leq 0.05$ were considered significant. The involvement of unigenes in metabolic and signaling pathways was discerned through the Kyoto Encyclopedia of Genes and Genomes (KEGG; https://www.genome.jp/kegg/) using the KOALA annotation tool.

Identification of simple sequence repeats (SSRs)

Microsatellite loci within the unigene dataset were identified using MISA software following the procedure described by [36]. SSR motifs of di-, tri-, tetra-, penta-, and hexanucleotide repeats with a minimum occurrence of five repeat units were catalogued for further analysis.

Detection of single-nucleotide polymorphisms (SNPs)

High-quality reads were aligned to the assembled transcriptome using the HISAT2 aligner [37] to facilitate the identification of sequence variants. SNPs were detected using the FreeBayes variant calling pipeline and filtered to include loci with a minimum read depth of three. Both biallelic and multiallelic SNPs identified across *P. sargentii*, *S. miamiensis*, and *S. palmetto* were functionally annotated using SNPEff with a custom-built reference database.

Results and discussion

Transcriptome sequencing and assembly

Table 1: The summary stats of raw and filtered reads from native palms.

Species	Raw reads	Filtered reads	% Filtered reads
Pseudophoenix sargentii	209,801,758	186,421,928	88.86
Sabal miamiensis	196,884,996	176,869,114	89.83
S. palmetto	248,270,724	213,661,114	86.06
Total	654,957,478	576,952,156	88.25

A total of 654,957,478 reads were generated across *P. sargentii, S. miamiensis,* and *S. palmetto* (Table 1). After quality filtering and adapter trimming, 576,952,156 high-quality reads were retained, corresponding to an average retention rate of 88.25%. The number of retained reads per species ranged from 176.9 million in *S. miamiensis* to 213.7 million in *S. palmetto.* The high retention rate (>86%) across all libraries indicate good sequencing quality and minimal adapter contamination.

Table 2: Summary statistics of the *de novo* transcriptome of native palm species.

	Raw assembly	Filtered assembly
Total contigs	455,094	82,949
Mean contig length	874	1577.89
Median contig length	829.5	409
Total contig length (nt)	397,599,596	130,884,010
Maximum contig Length (nt)	15,678	15,678
Minimum Contig Length (nt)	177	297
Number of non ATGC characters	0	0
Contigs >= 500b	225,994	71,432
Contigs >= 1kb	123,013	49,688
Contigs >= 10kb	72	35
N50	1,460	2,146
As (%)	29.29	28.15
Ts (%)	29.46	28.3
Gs (%)	20.48	21.7
Cs (%)	20.76	21.85
GC content (%)	41.12	45.34
Number of non-redundant unigenes		42,834

De novo assembly generated 455,094 contigs with a total assembled length of 397.6 Mbp (Table 2). The raw assembly exhibited a mean contig length of 874 bp, a median length of 829.5 bp, and an N50 of 1,460 bp. Following redundancy reduction and post-assembly filtering, the final assembly was substantially refined to 82,949 transcripts with a total length of 130.9 Mb. Assembly quality improved notably after filtering, as reflected by the increase in mean contig length to 1,577.9 bp and N50 to 2,146 bp, despite a reduction in overall contig number. The filtered assembly retained 42,834 non-redundant unigenes, representing a more compact and biologically meaningful transcript catalog.

Of the 42,834 non-redundant unigenes, 29,033 were detected in *P. sargentii*, 29,691 in S. *miamiensis*, and 28,337 in *S. palmetto* (Figure 1). The largest proportion of unigenes (16,218; 37.9%; Supplementary Table 1) were commonly shared among all three species, indicating a substantial core transcriptome conserved across these native palms. Species-specific expression was observed in each taxon, with 11,901 unigenes uniquely present in *P. sargentii*, 2,027 in *S. miamiensis*, and 897 in *S. palmetto*. In addition, 569 unigenes were shared exclusively between *P. sargentii* and *S. miamiensis*, 345 between *P. sargentii* and *S. palmetto*, and 10,877 between the two *Sabal* species, reflecting their closer phylogenetic relationship. The substantial overlap between *S. miamiensis* and *S. palmetto* further supports their genetic proximity, whereas the presence of species-specific unigenes may reflect lineage-specific adaptations or differential gene expression patterns.

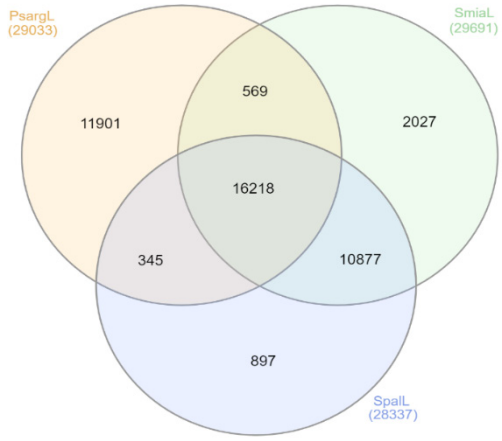

Figure 1: Dot plot of the enriched biological processes GO terms annotated to the DEUs in **(A)** *S. miamiensis* vs *P. sargentii,* **(B)** *S. miamiensis* vs *S. palmetto,* and **(C)** *S. palmetto* vs *P. sargentii*. The size of each dot is proportional to the number of genes associated with the corresponding GO term and color gradience is with respect to the *p*-value.

Pairwise differential expression analysis revealed clear transcriptional divergence among the three native palm species (Figure 2; Supplementary Table 2). The comparison between *S. miamiensis* and *P. sargentii* yielded 28,611 DEUs (14,473 upregulated and 14,138 downregulated) (Supplementary Table 3). In contrast, a total of 6,038 differentially expressed unigenes (DEUs) were identified between *S. miamiensis* and *S. palmetto*, including 2,191 upregulated and 3,847 downregulated transcripts (Supplementary Table 4). Similarly, the comparison between *S. palmetto* and *P. sargentii* identified 27,306 DEUs, comprising 12,692 upregulated and 14,614 downregulated transcripts (Supplementary Table 5). The substantially larger number of DEUs observed in comparisons involving *P. sargentii* indicates greater transcriptomic divergence between genera, whereas the relatively smaller number of DEUs between the two *Sabal* species reflects their closer evolutionary relationship and more conserved regulatory networks. The nearly balanced distribution of up- and downregulated genes in the intergeneric comparisons suggests extensive transcriptional reprogramming rather than a directional bias in gene regulation.

A total of 1,985 DEUs were shared across all comparisons, representing a core set of genes consistently differentiating the three species (Figure 3, Supplementary Table 2). The largest group of unique DEUs was detected in the *S. miamiensis* vs *P. sargentii* comparison (22,192), followed by 1,540 unique DEUs in *S. palmetto* vs *P. sargentii* and 319 unique DEUs in *S. miamiensis* vs *S. palmetto*. Additionally, 2,289 DEUs were shared exclusively between *S. miamiensis* vs *P. sargentii* and *S. miamiensis* vs *S. palmetto*, while 1,589 DEUs were shared between *S. palmetto* vs *P. sargentii* and *S. miamiensis* vs *S. palmetto*. Another 2,145 DEUs were common to the two comparisons involving *P. sargentii*. The relatively small number of unique and shared DEUs between the two *Sabal* species further supports their close transcriptional similarity, whereas the large number of unique DEUs associated with *P. sargentii* likely reflects genus-level divergence in gene regulation. Collectively, these results highlight both conserved and lineage-specific transcriptional signatures among the three native palm species.

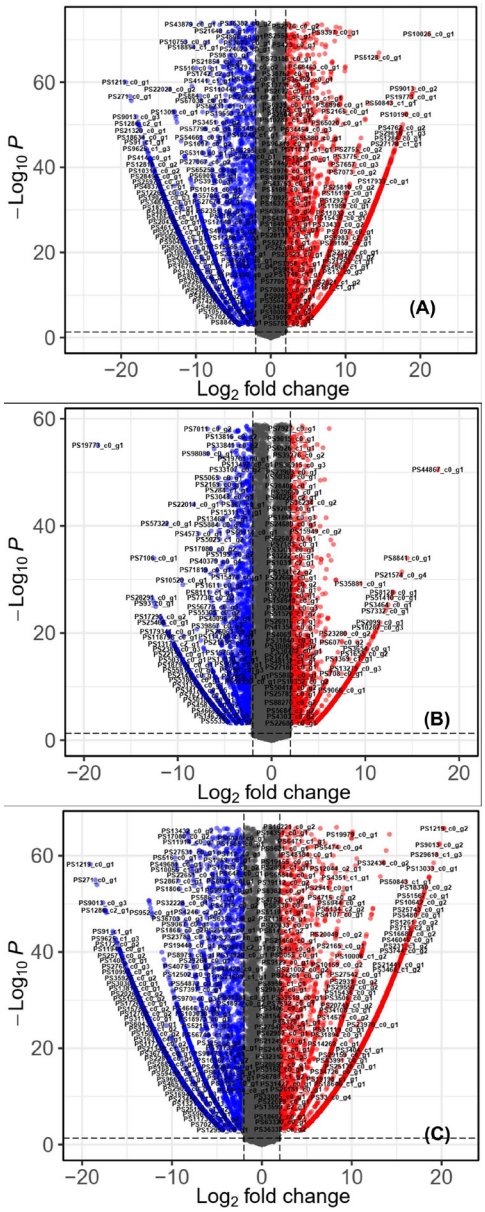

Figure 2: Volcano plot showing the Differentially Expressed Unigenes (DEUs) in **(A)** *S. miamiensis* vs *P. sargentii,* **(B)** *S. miamiensis* vs *S. palmetto,* and **(C)** *S. palmetto* vs *P. sargentii*. Black, red, and blue dots represent non-significant, significantly upregulated, and significantly downregulated DEUs, respectively, with - 2 ≤ log2FC ≥ 2 and -Log10*P* ≥ 1.3

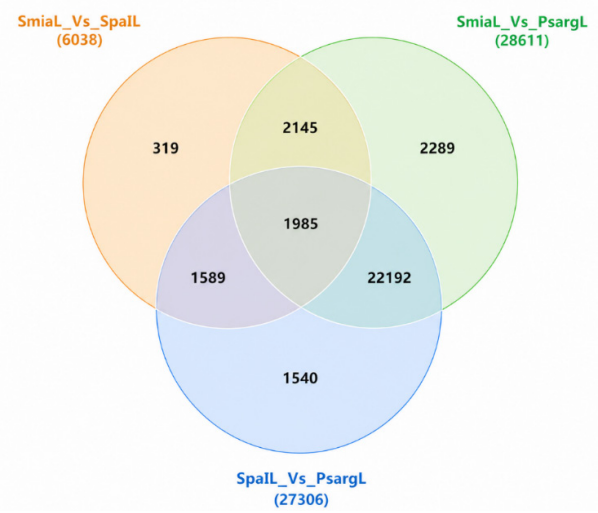

Figure 3: Venn diagram showing the number of Differentially Expressed Unigenes (DEU) among the native palms.

Gene ontology enrichment analysis of DEUs

Gene Ontology (GO) enrichment analysis of DEUs revealed coordinated functional divergence among *S. miamiensis*, *S. palmetto*, and *P. sargentii* (Figure 4, Supplementary Figure 1 and Supplementary Figure 2). Across all pairwise comparisons, enriched categories primarily involved biological processes associated with biosynthesis, translation, nucleic acid metabolism, and stress-related pathways, consistent with patterns reported in comparative transcriptomic studies of non-model plant species [38,39].

Biological processes

In the *S. miamiensis* vs *P. sargentii* comparison, upregulated DEUs were significantly enriched in organic substance biosynthetic process (GO:1901576), organonitrogen compound biosynthetic process (GO:1901566), cellular biosynthetic process (GO:0044249), peptide biosynthetic process (GO:0043043), amide biosynthetic process (GO:0043604), ribosome assembly (GO:0042255), and translation (GO:0006412) (Figure 4A, Supplementary Table 3). Downregulated DEUs were enriched in nucleic acid metabolic process (GO:0090304), DNA metabolic process (GO:0006259), DNA replication (GO:0006260), DNA-dependent DNA replication (GO:0006261), DNA repair (GO:0006281), and RNA modification (GO:0009451). Similar trends were observed in *S. palmetto* vs *P. sargentii*, where defense response to other organism (GO:0098542), immune response (GO:0006955), and regulation of nucleic acid-templated transcription (GO:1903506) were prominent among upregulated DEUs, while DNA metabolic and replication-related processes were enriched among downregulated transcripts (Figure 4C).

In contrast, the comparison between the two *Sabal* species showed relatively stronger enrichment of translational and ribosome-related processes among downregulated DEUs, including ribosome biogenesis (GO:0042254), gene expression (GO:0010467), and plant-type cell wall organization (GO:0009664), whereas upregulated DEUs were associated with amino acid catabolic processes (GO:0009065) and small molecule metabolic processes (GO:0044282) (Figure 4B, Supplementary Table 4). These findings suggest that divergence between genera is characterized by broader shifts in transcriptional regulation and defense-associated pathways, while interspecific variation within *Sabal* is driven primarily by metabolic and translational modulation.

Cellular components

Enriched cellular component terms further supported these patterns. Comparisons involving *P. sargentii* showed significant enrichment of ribosome (GO:0005840), cytosolic ribosome (GO:0022626), ribosomal subunit (GO:0044391), cytoplasm (GO:0005737), and plasma membrane (GO:0005886) among upregulated DEUs (Supplementary Figure 1A, 1C, Supplementary Table 3, 5). Downregulated transcripts were enriched in membrane-bounded organelle (GO:0043227), nucleus (GO:0005634), nuclear lumen (GO:0031981), and cytoskeleton (GO:0005856), indicating shifts in subcellular compartmental activity.

Between *S. miamiensis* and *S. palmetto*, enrichment of extracellular region (GO:0005576), cell wall (GO:0005618), and membrane-associated components (GO:0016020) were observed, suggesting structural and membrane-related divergence within the genus (Supplementary Figure 1B). Such compartment-level differences have been widely reported in comparative plant transcriptome analyses, particularly in studies investigating stress adaptation and lineage differentiation [25,40].

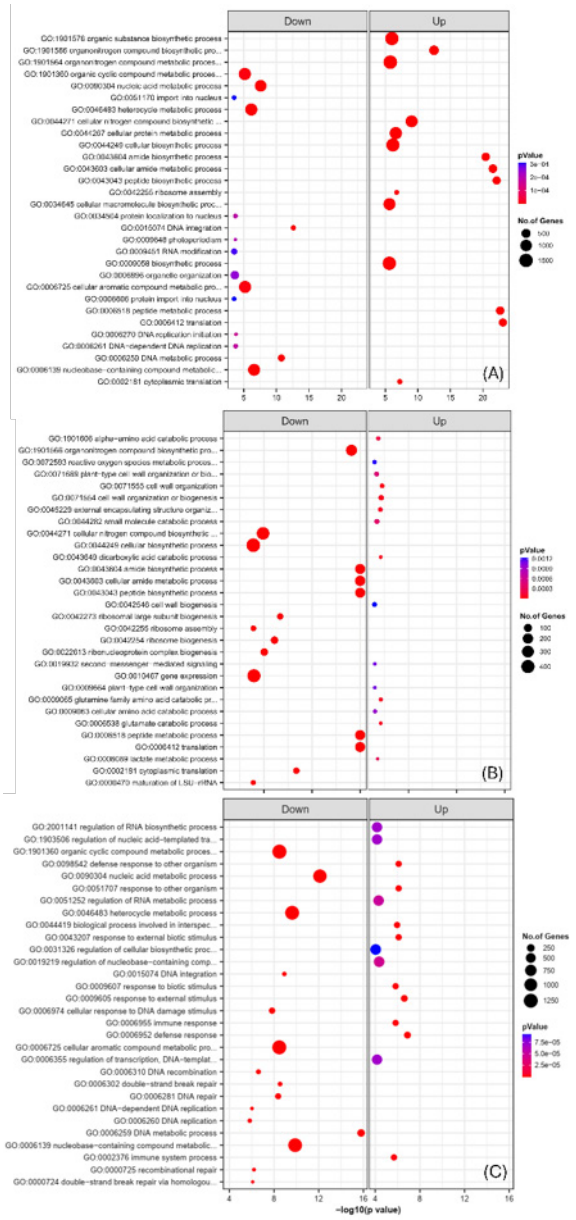

Figure 4: Dot plot of the enriched biological processes GO terms annotated to the DEUs in **(A)** *S. miamiensis* vs *P. sargentii,* **(B)** *S. miamiensis* vs *S. palmetto,* and **(C)** *S. palmetto* vs *P. sargentii*. The size of each dot is proportional to the number of genes associated with the corresponding GO term and color gradience is with respect to the *p*-value.

Molecular functions

At the molecular function level, catalytic activity (GO:0003824), oxidoreductase activity (GO:0016491), nucleic acid binding (GO:0003676), DNA-binding transcription factor activity (GO:0003700), and transcription regulator activity (GO:0140110) were recurrently enriched across comparisons (Supplementary Figure 2, Supplementary Table 5). Intergeneric contrasts consistently showed stronger enrichment of transcription factor and DNA-binding functions, along with oxidoreductase and monooxygenase activities (GO:0004497), suggesting greater regulatory and metabolic differentiation between *Sabal* and *Pseudophoenix* (Supplementary Figure 2A, 2C). Downregulated DEUs were frequently associated with ATP-dependent activity (GO:0140657), helicase activity (GO:0004386), and single-stranded DNA binding (GO:0003697), indicating modulation of genome maintenance and nucleic acid processing pathways.

Collectively, the integrated Biological Processes (BP), Cellular Components (CC), and Molecular Functions (MF) enrichment patterns demonstrate that transcriptomic divergence among these native palms is largely driven by coordinated shifts in biosynthetic activity, protein synthesis, transcriptional regulation, redox processes, and defense-related mechanisms. Comparisons involving *P. sargentii* showed stronger enrichment of regulatory and immune-associated functions, supporting greater functional divergence at the genus level relative to the two closely related *Sabal* species. Environmental stressors such as salinity and coastal habitat conditions are known to influence physiological responses in native palms, including *S. palmetto* and *P. sargentii*, potentially contributing to divergence in gene expression patterns [41]. Such enrichment trends are consistent with previous *de novo* transcriptome studies in non-model plants, where differential regulation of translation, metabolic pathways, and stress-responsive genes underpins species-level adaptation [38,39].

A set of representative DEUs revealed consistent transcriptional divergence among *S. miamiensis*, *S. palmetto*, and *P. sargentii* in leaf tissue (Table 3). Among the DEUs expressed in all three pairwise comparisons, several genes associated with phenylpropanoid and secondary metabolism exhibited strong and consistent differential expression across all contrasts (Table 3A). Trans-cinnamate 4-monooxygenase (PS1536_c0_g2) and a 2-oxoglutarate/iron-dependent dioxygenase (PS12726_c0_g1) showed substantial log2FC values in each comparison, indicating coordinated divergence in phenylpropanoid flux. C4H catalyzes an early committed step in phenylpropanoid biosynthesis and regulates lignin and flavonoid production [42,43]. The 2-oxoglutarate-dependent dioxygenase superfamily plays broad roles in flavonoid modification and specialized metabolism [44], suggesting that secondary metabolite allocation differs among the three taxa.

Cell wall and redox-associated differences were further supported by the differential expression of a multi-copper oxidase (PS17938_c0_g1) and an anchored cell wall protein (PS89637_c0_g1). Laccase-type multi-copper oxidases are central to lignin polymerization and structural reinforcement of the cell wall [45], while apoplastic redox enzymes modulate oxidative balance in expanding tissues. The coordinated shifts observed in these transcripts imply divergence in structural and redox homeostasis among the species.

Table 3: Selected Differentially Expressed Unigenes (DEUs) distinguishing native palm species, **(A)** DEUs shared across all pairwise comparisons, **(B)** DEUs shared in both *Sabal-Pseudophoenix* comparisons.

	S. miamiensis* vs *P. sargentii		***S. miamiensis* vs *S. palmetto***		***S. palmetto* vs *P. sargentii***		
Unigene ID	**Log2FC**	**padj**	**Log2FC**	**padj**	**Log2FC**	**padj**	**Annotation**
A							
PS12726_c0_g1	13.71	1.03E-30	-7.14	2.14E-231	6.61	7.73E-08	2-oxoglutarate/iron-dependent dioxygenase
PS41483_c0_g1	9.91	1.04E-16	-5.22	1.99E-33	4.73	0.0003	Rust resistance kinase LR10-related
PS38151_c0_g1	5.24	2.00E-05	6.58	3.20E-93	11.86	2.64E-23	Acid phosphatase-like protein
PS28026_c0_g1	-12.34	3.91E-25	6.11	1.70E-06	-6.18	5.48E-126	Myo-inositol oxygenase
PS1536_c0_g2	6.34	1.57E-07	5.99	5.28E-162	12.37	3.13E-25	Trans-cinnamate 4-monooxygenase (C4H)
PS89637_c0_g1	4.44	4.00E-04	5.82	1.49E-41	10.29	7.37E-18	Anchored cell wall protein
PS1824_c0_g2	-5.72	6.25E-122	-5.77	6.28E-06	-11.45	8.36E-22	Acetylornithine deacetylase
PS17938_c0_g1	11.52	4.40E-22	-5.66	1.66E-87	5.9	2.43E-06	Multi-copper oxidase (laccase/ascorbate oxidase family)
PS34528_c0_g1	10.28	6.89E-18	-5.59	1.11E-38	4.73	3.00E-04	Auxin-responsive protein IAA17 (AUX/IAA family)
PS28858_c0_g1	10.4	2.82E-18	-5.39	1.99E-44	5.06	9.95E-05	LRR receptor-like serine/threonine kinase (ERECTA-like)
B							
PS1219_c0_g1	-19.37	4.79E-60			-19.07	3.08E-58	Photosystem II 22 kDa protein, chloroplastic
PS32264_c0_g1	18.8	1.28E-56			13.91	1.52E-31	Naringenin,2-oxoglutarate 3-dioxygenase
PS1_c0_g1	-18.64	1.04E-55			-18.34	5.70E-54	BURP domain protein USPL1-like
PS10190_c0_g1	18.09	1.53E-52			13.7	1.19E-30	Flavonol synthase
PS9013_c0_g3	-17.98	6.12E-52			-17.69	2.91E-50	Calvin cycle protein CP12-2, chloroplastic
PS3964_c0_g2	-17.67	3.60E-50			-17.37	1.60E-48	Carbonic anhydrase
PS18340_c0_g2	16.12	5.69E-42			18.25	1.84E-53	Peroxiredoxin (thioredoxin domain/redoxin)
PS19504_c0_g1	17.09	5.00E-47			18.6	1.87E-55	Protochlorophyllide reductase C
PS11494_c0_g3	15.4	1.96E-38			18.61	1.61E-55	Ferredoxin (2Fe-2S)
PS251_c2_g1	17.47	4.25E-49			16.01	2.00E-41	Annexin

Regulatory divergence was also evident at the signaling level. An auxin-responsive protein IAA17 (PS34528_c0_g1) was significantly differentially expressed in all three comparisons, indicating variation in auxin signaling regulation. AUX/IAA proteins act as transcriptional repressors within auxin response pathways and integrate growth and stress signaling [46]. Similarly, an ERECTA-like LRR receptor-like serine/threonine kinase (PS28858_c0_g1) and an LR10-related rust resistance kinase (PS41483_c0_g1) were differentially expressed across contrasts. ERECTA-family receptor kinases are known to coordinate

developmental patterning and environmental responses [47], while LRR receptor kinases broadly mediate pathogen perception and downstream defense signaling. These findings suggest divergence in upstream perception and hormonal regulatory circuits in addition to downstream metabolic processes.

Nutrient and nitrogen-associated metabolism also contributed to species differentiation. An acid phosphatase-like protein (PS38151_c0_g1) displayed strong differential expression across comparisons, consistent with variation in phosphate remobilization and nutrient-use strategies [48]. Additionally, acetylornithine deacetylase (PS1824_c0_g2), involved in arginine biosynthesis, showed consistent differential expression, implicating divergence in nitrogen metabolism. Arginine metabolism is closely linked to nitrogen storage and stress responses in plants [49]. Differential expression of myo-inositol oxygenase (PS28026_c0_g1) further indicates variation in carbohydrate metabolism and cell wall precursor pathways.

Among the genes consistently differentiating *Sabal* species from *P. sargentii*, several chloroplast-associated genes, including photosystem II 22 kDa protein (PS1219_c0_g1), CP12-2 (PS9013_c0_g3), protochlorophyllide reductase C (PS19504_c0_g1), and ferredoxin (PS11494_c0_g3), exhibited strong differential expression in both *Sabal-Pseudophoenix* contrasts (Table 3B). Chloroplast redox components such as ferredoxin and peroxiredoxin (PS18340_c0_g2) play central roles in photosynthetic electron transport and reactive oxygen species buffering [50,51], indicating divergence in photosynthetic regulation and redox balance between genera. In parallel, flavonoid-associated genes such as flavonol synthase (PS10190_c0_g1) and naringenin 2-oxoglutarate 3-dioxygenase (PS32264_c0_g1) were consistently elevated in *Sabal* relative to *Pseudophoenix*, reinforcing divergence in photoprotective secondary metabolism [43,44]. Finally, annexin (PS251_c2_g1), a calcium-dependent membrane-associated protein implicated in stress and signaling processes [52], further supports genus-level differences in signaling and membrane-associated stress responses.

Collectively, these DEUs indicate coordinated divergence in phenylpropanoid metabolism, cell wall and redox homeostasis, hormone and receptor-mediated signaling, chloroplast physiology, and nutrient metabolism. Such integration of metabolic and regulatory differentiation is consistent with comparative transcriptomic studies in other plant systems, where species-level divergence reflects coordinated shifts in signaling networks and downstream metabolic pathways [53,54]. The selected DEUs therefore provide biologically meaningful candidate loci underlying functional differentiation among these native palm species.

Identification and characterization of SSRs in native palm transcriptome

Simple Sequence Repeats (SSRs) analysis identified 10,145 SSR loci from 42,834 assembled transcript sequences, representing a total sequence length of 55,381,788 bp (Table 4). Among these sequences, 14,384 transcripts contained at least one SSR, while 5,029 sequences harbored more than one SSR, indicating the widespread distribution of microsatellites across the transcriptome. Such abundance of SSRs within expressed regions has been commonly reported in plant transcriptome datasets and provides valuable resources for marker development and genetic studies [55,56].

Among the identified SSRs, dinucleotide repeats were the most abundant (5,752), followed by trinucleotide repeats (3,960), while tetranucleotide (332), pentanucleotide (55), and hexanucleotide repeats (46) were comparatively rare (Table 4). Similar patterns have been widely reported in plant EST or transcriptome-derived SSR studies, where di- and trinucleotide repeats typically dominate due to their relative mutational stability and frequent occurrence in coding regions [55,57]. In the present study, dinucleotide and trinucleotide repeats together accounted for 95.73% of the total SSRs, suggesting their major contribution to microsatellite variation within the native palm transcriptome.

Table 4: Summary statistics of SSR and SNP identification in native palms.

Parameter	Value
SSR identification	
Total number of sequences examined	42,834
Total size of examined sequences (bp)	55,381,788
Total number of identified SSRs	10,145
Dinucleotide repeat motif SSRs	5,752 (56.70%)
Trinucleotide repeat motif SSRs	3,960 (39.03%)
Tetranucleotide repeat motif SSRs	332 (3.27%)
Pentanucleotide repeat motif SSRs	55 (0.54%)
Hexanucleotide repeat motif SSRs	46 (0.45%)
Class-I (motif length ≥ 20bp) SSRs	4,062 (40.03%)
Class-II (motif length ≥ 10bp and < 20bp) SSRs	6,083 (59.96%)
Number of complex SSRs	34
SNP identification	
Number of Transcripts with SNPs	8,571
Number of SNPs	23,876
Average SNPs per transcript	2.78
PS9893_C0_G1_I4 (transcript with maximum SNPs)	25
Transcripts with Single SNP	3,406
Number of Transversions	7,361
Number of Transitions	16,515
Transition/transversion ratio	2.24

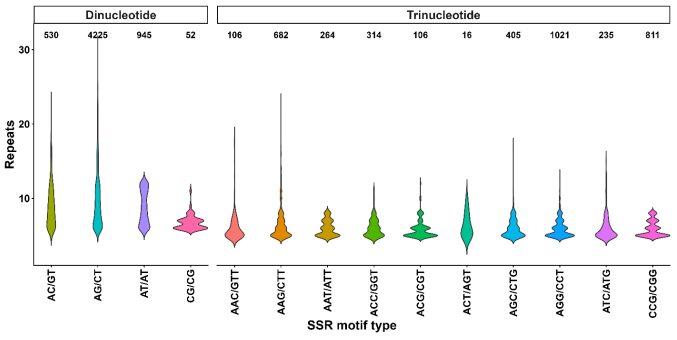

Figure 5: Repeat number distribution of dinucleotide and trinucleotide SSR motif types identified in native palms.

SSRs were further classified based on motif length into Class-I SSRs (≥20 bp) and Class-II SSRs (10–20 bp). A total of 4,062 Class-I SSRs (40.03%) and 6,083 Class-II SSRs (59.96%) were detected (Table 4). Class-II SSRs were therefore more prevalent than Class-I SSRs, which is consistent with observations from other transcriptome-based SSR analyses where shorter repeat

motifs are generally more frequent [56,58]. Only 34 SSRs occurred in compound formation, indicating that most SSR loci consisted of simple repeat motifs.

The study of distribution of SSR lengths across different motif types showed dinucleotide repeats an average length of 26.19 bp in Class-I SSRs and 14.40 bp in Class-II SSRs, while trinucleotide repeats exhibited average lengths of 23.90 bp and 16.04 bp in Class-I and Class-II categories, respectively (Supplementary Table 6). Tetranucleotide, pentanucleotide, and hexanucleotide repeats were observed exclusively within the Class-I category with average motif lengths of 24.0 bp, 26.41 bp, and 34.9 bp, respectively.

The predominance of longer motifs within higher-order repeat classes is expected because larger motif units require fewer repeat iterations to meet the minimum length threshold for classification as SSRs. Similar length patterns have been reported in transcriptome-derived SSR analyses of several plant species including coffee, *Morinda officinalis*, and *Spartina alterniflora* [29,59,60]. In our study, hexanucleotide repeats exhibited the largest average length, which likely reflects their lower abundance but higher repeat stability within coding regions.

Considerable variation in repeat numbers was observed across motif types (Figure 5). Among dinucleotide repeats, motifs such as AG/CT and AC/GT exhibited the highest frequencies, indicating their strong prevalence within the transcriptome. In trinucleotide repeats, motifs such as AAG/CTT, AAT/ATT, and AGG/CCT were among the most frequent types. The predominance of AG/CT-type dinucleotide motifs and AAG/CTT-type trinucleotide motifs have been consistently reported across many plant species. For example, similar motif patterns were observed in coffee and *Morinda officinalis*, where AG/CT dinucleotide repeats were the most abundant SSR motifs [59,60]. The high frequency of trinucleotide repeats in transcriptomic sequences is often attributed to their compatibility with coding regions because they do not disrupt the reading frame during replication slippage events [56]. Most SSR motifs exhibited repeat numbers ranging from approximately 5 to 12 repeat units, with a few motifs showing higher repeat counts. Previous genetic studies have demonstrated considerable genetic variation within *P. sargentii* populations using microsatellite markers, suggesting that genomic variability may also contribute to observed transcriptional differences among related palm taxa [61]. Such variability in repeat number is a characteristic feature of microsatellites and contributes to their high level of polymorphism, making them valuable molecular markers for genetic diversity studies and marker-assisted breeding.

Identification and characterization of SNPs in native palm transcriptome

Single Nucleotide Polymorphisms (SNPs) were identified from the assembled transcriptome sequences to evaluate nucleotide-level variation among the native palm datasets. A total of 23,876 SNPs were detected across 8,571 transcripts, resulting in an average of 2.78 SNPs per transcript (Table 4). The transcript PS9893_C0_G1_I4 contained the highest number of SNPs, with 25 variants, indicating localized regions of high nucleotide variability within the transcriptome.

Among the identified SNPs, 16,515 were transitions, while 7,361 were transversions (Supplementary Table 7), resulting in a Transition/Transversion (Ti/Tv) ratio of 2.24. The predominance of transitions over transversions is consistent with observations from many plant transcriptome studies, where transitions typically occur more frequently due to the higher likelihood of purine–purine and pyrimidine–pyrimidine substitutions during DNA replication and repair processes [55,56,62]. In addition, 3,406 transcripts contained a single SNP, indicating that a large proportion of transcripts harbor limited nucleotide variation, while others accumulate multiple polymorphic sites. The distribution of SNPs across transcripts reflects both functional constraints on coding sequences and the natural mutational processes shaping genetic variation in plant genomes. Transcriptome-derived SNPs are particularly valuable as potential markers because they originate from expressed genes and may therefore be directly associated with functional traits or adaptive responses [55,62].

Conclusion

This study provides the first comprehensive transcriptomic characterization of three native Florida palm species, *P. sargentii*, *S. miamiensis*, and *S. palmetto*, offering new insights into their genetic architecture and transcriptional divergence. Comparative transcriptome analysis revealed conserved and species-specific gene expression patterns associated with metabolic regulation, stress response, and developmental processes, highlighting potential molecular mechanisms underlying ecological adaptation among these native palms. The transcriptome resources generated in this work substantially expand the currently limited genomic information available for Florida's native palm species and establish an important foundation for future functional genomics and conservation studies. These datasets also provide valuable genetic resources that can facilitate germplasm characterization, molecular marker development, species restoration, and marker-assisted breeding efforts aimed at improving resilience and sustainability in ornamental palm cultivation as well as conservation biology.

Author declarations

Acknowledgements

This research was supported through appropriated funds from the United States Department of Agriculture - Agricultural Research Service (USDA-ARS) under Project Number 6038-13210-004-000-D and study conducted under Non-Assistance Cooperative Agreement (6038-21000-026-006-S). This research was supported by an appointment to the Agricultural Research Service (ARS) Research Participation Program at the U.S. Department of Agriculture (USDA), administered by the Oak Ridge Institute for Science and Education (ORISE) through an interagency agreement between the U.S. Department of Energy (DOE) and the USDA-ARS.

Authors' contributions

MNR, PG, and VMG analyzed and visualized the data and drafted the manuscript. MNR, DT, and AK conducted field collections, obtained permits, and supported experimental work and literature review. MNR and NB performed quality control, data analysis and investigations, as well as manuscript editing. All authors reviewed and approved the final manuscript. MNR acquired USDA-ARS funding, NB obtained NACA funding and provided logistical support. The authors declare no competing interests.

References

1. UF-IFAS. TREC Plant Diagnostic Clinic: Keeping Florida's Diverse Horticulture Industry Healthy. 2019. https://www.newswise.com/articles/ufifas-trec-plant-diagnostic-clinic-keeping-florida-s-diverse-horticulture-industry-healthy
2. Florida Department of Agriculture. Overview and statistics. 2021. https://www.fdacs.gov/Agriculture-Industry/Florida-Agriculture-Overview-and-Statistics
3. Broschat TK, Meerow AW, Miller J. Field Production of Palms: ENH1210/EP471. EDIS. 2013; 2013.
4. Gonzalez PD, Tucker DA, Nageswara-Rao M, Griffith MP, Sridhar BBM, Ross M, et al. Enhancing cabbage palm resilience to saltwater stress through silicon applications. HortScience. 2025; 60: 1547-1554.
5. Miami Beach Urban Forestry Master Plan. Miami Beach Rising Above. 2020. 2020-CMB-UFMP-Final-compressed.pdf (mbrisingabove.com)
6. Miller K. Oaks instead of palm trees? Florida's iconic palms don't cut it with climate change. 2019. https://www.wusf.org/environment/2019-11-15/oaks-instead-of-palm-trees-floridas-iconic-palms-dont-cut-it-with-climate-change
7. Vaishali G, Nageswara-Rao M, Patrick G, Tucker DA, Singh S. Transcriptomic Insights into Salinity Responses in *Roystonea oleracea* Under Freshwater and Saline Field Conditions. J Plant Biol Crop Res. 2026; 10:1113.
8. Vaishali G, Nageswara-Rao M. Species-Associated Transcriptional Divergence in *Phoenix theophrasti* and *Phoenix pusilla*. J Plant Biol Crop Res. 2026; 10:1114.
9. Nair PR, Mohan Kumar B, Naresh Kumar S. Climate change, carbon sequestration, and coconut-based ecosystems. In: The Coconut Palm (*Cocos nucifera* L)-Research and Development Perspectives. Singapore: Springer. 2019; 779-799.
10. Broschat TK, Meerow AW, Elliott ML. Ornamental Palm Horticulture. 2nd ed. Gainesville, FL: University Press of Florida. 2017.
11. Williams E. Our mighty palm trees. 2018. https://www.floridaweekly.com/articles/palm-beach/our-mighty-palm-trees/
12. Florida Exotic Pest Plant Council (FLEPPC). 2021. https://www.floridainvasives.org/
13. Rubenstein KD, Heisey PW. Developing country demand for crop germplasm conserved by the US National Plant Germplasm System. CABI Agric Biosci. 2022; 3: 16.
14. Araújo MB, Alagador D, Cabeza M, Nogués-Bravo D, Thuiller W. Climate change threatens European conservation areas. Ecol Lett. 2011; 14: 484-492.
15. Stys B, Foster T, Fuentes MMPB, Glazer B, Karish K, et al. Climate change impacts on Florida's biodiversity and ecology. Florida›s Climate: Changes, Variations & Impacts. 2017; 339-388.
16. Allyn A. Florida's native palms. Pinellas Chapter FNPS-Florida Native Plant Society. 2021. https://pinellas.fnpschapters.org/native-plant-profiles/palms/
17. Anderson P. Native Palms of Florida: Identification and Regulation. Botany Circular No. 41. Florida Department of Agriculture and Consumer Services. 2019. https://www.fdacs.gov/About-Us/Publications/Plant-Industry-Publications/Botany-Circulars
18. Pedro G, Tucker D, Nageswara-Rao M, Sridhar BBM, Griffith P, et al. Enhancing Cabbage Palm Resilience to Saltwater Stress through Silicon Applications. HortScience. 2025; 60: 1547-1554.
19. Tucker DA, Sanín MJ, Griffith MP, Valenzuela S, Nuñez L, Khoddamzadeh AA. *Sabal miamiensis:* Discovery of a new wild population and restoration efforts. Palms. 2025; 69: 177-182.
20. Butler CJ, Larson M. Climate change winners and losers: The effects of climate change on five palm species in the Southeastern United States. Ecol Evol. 2020; 10: 10408-10425.
21. Kuchta DM. The problem with Florida palm trees: native vs non-native palms. 2021. https://www.treehugger.com/florida-palm-trees-5210417
22. Tucker DA, Noblick LR, Joyner T. *Sabal miamiensis*: Not Extinct in the Wild. Palms. 2024; 68(1): 11-13.
23. Reeve AB. Phylogenomics of the Roystonea Genus, the Royal Palms of the Caribbean. Doctoral dissertation. University of Miami. 2023.
24. Vaishali G, Nageswara-Rao M, Govindarajulu G, Meerow AW, Singh S. Genetic Insights into *Amaryllidaceae* Species: A Comparative Transcriptomic Analysis. J Biosci. 2025; 50:82.
25. Grabherr MG, Haas BJ, Yassour M, Levin JZ, Thompson DA, et al. Trinity: reconstructing a full-length transcriptome without a genome from RNA-Seq data. Nat Biotechnol. 2011; 29: 644-652.
26. Haas BJ, Papanicolaou A, Yassour M, Grabherr M, Blood PD, et al. *De novo* transcript sequence reconstruction from RNA-seq using the Trinity platform for reference generation and analysis. Nat Protoc. 2013; 8: 1494-1512.
27. Raghavan V, Kraft L, Mesny F, Rigerte L. A simple guide to *de novo* transcriptome assembly and annotation. Brief Bioinform. 2022; 23: bbab563.
28. Yan WJ, Pendi FH, Hussain H. Improved CTAB method for RNA extraction of thick waxy leaf tissues from sago palm. Chem Biol Technol Agric. 2022; 9: 63.
29. Bedre R, Mangu VR, Srivastava S, Sanchez LE, Baisakh N. Transcriptome analysis of smooth cordgrass (*Spartina alterniflora* Loisel), a monocot halophyte reveals candidate genes involved in adaptation to salinity. BMC Genomics. 2016; 17: 657.
30. Gandham P, Rajasekaran K, Sickler C, Mohan H, Gilbert M, et al. MicroRNA profiling of maize genotypes with differential response to *Aspergillus flavus* implies resistance mechanisms. Stress Biol. 2024; 4: 26.
31. Bolger AM, Lohse M, Usadel B. Trimmomatic: a flexible trimmer for Illumina sequence data. Bioinformatics. 2014; 30: 2114-2120.
32. Fu L, Niu B, Zhu Z, Wu S, Li W. CD-HIT: accelerated for clustering the next-generation sequencing data. Bioinformatics. 2012; 28: 3150-3152.
33. Kalvari I, Nawrocki EP, Ontiveros-Palacios N, Argasinska J, Lamkiewicz K, et al. Rfam 14: expanded coverage of metagenomic viral and microRNA families. Nucleic Acids Res. 2021; 49: D192-D200.
34. Li B, Dewey CN. RSEM: accurate transcript quantification from RNA-Seq data with or without a reference genome. BMC Bioinformatics. 2011; 12: 323.
35. Love MI, Huber W, Anders S. Moderated estimation of fold change and dispersion for RNA-seq data with DESeq2. Genome Biol. 2014; 15: 550.
36. Beier S, Thiel T, Münch T, Scholz U, Mascher M. MISA-web: a web server for microsatellite prediction. Bioinformatics. 2017; 33: 2583-2585.

37. Kim D, Paggi JM, Park C, Bennett C, Salzberg SL. Graph-based genome alignment and genotyping with HISAT2 and HISAT-genotype. Nat Biotechnol. 2019; 37: 907-915.

38. Wang Z, Gerstein M, Snyder M. RNA-Seq: a revolutionary tool for transcriptomics. Nat Rev Genet. 2009; 10: 57-63.

39. Conesa A, Madrigal P, Tarazona S, Gomez-Cabrero D, Cervera A, et al. A survey of best practices for RNA-seq data analysis. Genome Biol. 2016; 17: 13.

40. Mutz KO, Heilkenbrinker A, Lönne M, Walter JG, Stahl F. Transcriptome analysis using next-generation sequencing. Curr Opin Biotechnol. 2013; 24: 22-30.

41. Khoddamzadeh AA, Flores J, Griffith MP, Souza Costa BN. Saltwater intrusion ecophysiological effects on *Pseudophoenix sargentii*, *Roystonea regia*, *Sabal palmetto* 'Lisa' and *Thrinax radiata* in South Florida. Front Ecol Evol. 2023; 11:1127679.

42. Bell-Lelong DA, Cusumano JC, Meyer K, Chapple C. Cinnamate-4-hydroxylase expression in Arabidopsis (regulation in response to development and the environment). Plant Physiol. 1997; 113: 729-738.

43. Vogt T. Phenylpropanoid biosynthesis. Mol Plant. 2010; 3: 2-20.

44. Kawai Y, Ono E, Mizutani M. Evolution and diversity of the 2-oxoglutarate-dependent dioxygenase superfamily in plants. Plant J. 2014; 78: 328-343.

45. Berthet S, Demont-Caulet N, Pollet B, Bidzinski P, Cézard L, et al. Disruption of LACCASE4 and 17 results in tissue-specific alterations to lignification of *Arabidopsis thaliana* stems. Plant Cell. 2011; 23: 1124-1137.

46. Li H, Cheng Y, Murphy A, Hagen G, Guilfoyle TJ. Constitutive repression and activation of auxin signaling in *Arabidopsis*. Plant Physiol. 2009; 149: 1277-1288.

47. Jordá L, Sopeña-Torres S, Escudero V, Nuñez-Corcuera B, Delgado-Cerezo M, et al. ERECTA and BAK1 receptor like kinases interact to regulate immune responses in *Arabidopsis*. Front Plant Sci. 2016; 7: 897.

48. Tran HT, Qian W, Hurley BA, SHE YM, Wang D, Plaxton WC. Biochemical and molecular characterization of AtPAP12 and AtPAP26. Plant Cell Environ. 2010; 33: 1789-1803.

49. Winter G, Todd CD, Trovato M, Forlani G, Funck D. Physiological implications of arginine metabolism in plants. Front Plant Sci. 2015; 6:534.

50. Dietz KJ, Turkan I, Krieger-Liszkay A. Redox- and reactive oxygen species-dependent signaling into and out of the photosynthesizing chloroplast. Plant Physiol. 2016; 171: 1541-1550.

51. Liebthal M, Maynard D, Dietz KJ. Peroxiredoxins and redox signaling in plants. Antioxid Redox Signal. 2018; 28: 609-624.

52. Clark GB, Morgan RO, Fernandez MP, Roux SJ. Evolutionary adaptation of plant annexins has diversified their molecular structures, interactions and functional roles. New Phytol. 2012; 196: 695-712.

53. Koenig D, Jiménez-Gómez JM, Kimura S, Fulop D, Chitwood DH, et al. Comparative transcriptomics reveals patterns of selection in domesticated and wild tomato. Proc Natl Acad Sci USA. 2013; 110: E2655-E2662.

54. Singh R, Ong-Abdullah M, Low ETL, Manaf MAA, Rosli R, et al. Oil palm genome sequence reveals divergence of interfertile species in Old and New worlds. Nature. 2013; 500: 335-339.

55. Varshney RK, Graner A, Sorrells ME. Genic microsatellite markers in plants: features and applications. Trends Biotechnol. 2005; 23: 48-55.

56. Kalia RK, Rai MK, Kalia S, Singh R, Dhawan AK. Microsatellite markers: an overview of the recent progress in plants. Euphytica. 2011; 177: 309-334.

57. Luro FL, Costantino G, Terol J, Argout X, Allario T, et al. Transferability of the EST-SSRs developed on Nules clementine to other Citrus species and their effectiveness for genetic mapping. BMC Genomics. 2008; 9: 287.

58. Temnykh S, DeClerck G, Lukashova A, Lipovich L, Cartinhour S, McCouch S. Computational and experimental analysis of microsatellites in rice (*Oryza sativa* L). Genome Res. 2001; 11: 1441-1452.

59. Poncet V, Rondeau M, Tranchant C, Cayrel A, Hamon S, et al. SSR mining in coffee tree EST databases: potential use of EST-SSRs as markers for the Coffea genus. Mol Genet Genomics. 2006; 276: 436-449.

60. Liao B, Lee SY, Meng K, Yin Q, Huang C, et al. Characterization and novel EST-SSR marker development of an important Chinese medicinal plant *Morinda officinalis* How (Rubiaceae). Biotechnol Biotechnol Equip. 2019; 33: 1311-1318.

61. Namoff S, Francisco-Ortega J, Zona S, Lewis C. Microsatellite markers developed for the Caribbean palm *Pseudophoenix sargentii*. Conserv Genet Resour. 2010; 2: 85-87.

62. Gandham P, Nageswara-Rao M, Singh S, Baisakh N. Comparative transcriptome analysis of *Portlandia* species reveals differences in the expression of genes involved in flower color and fragrance. Trop Plant Biol. 2025; 18: 66.

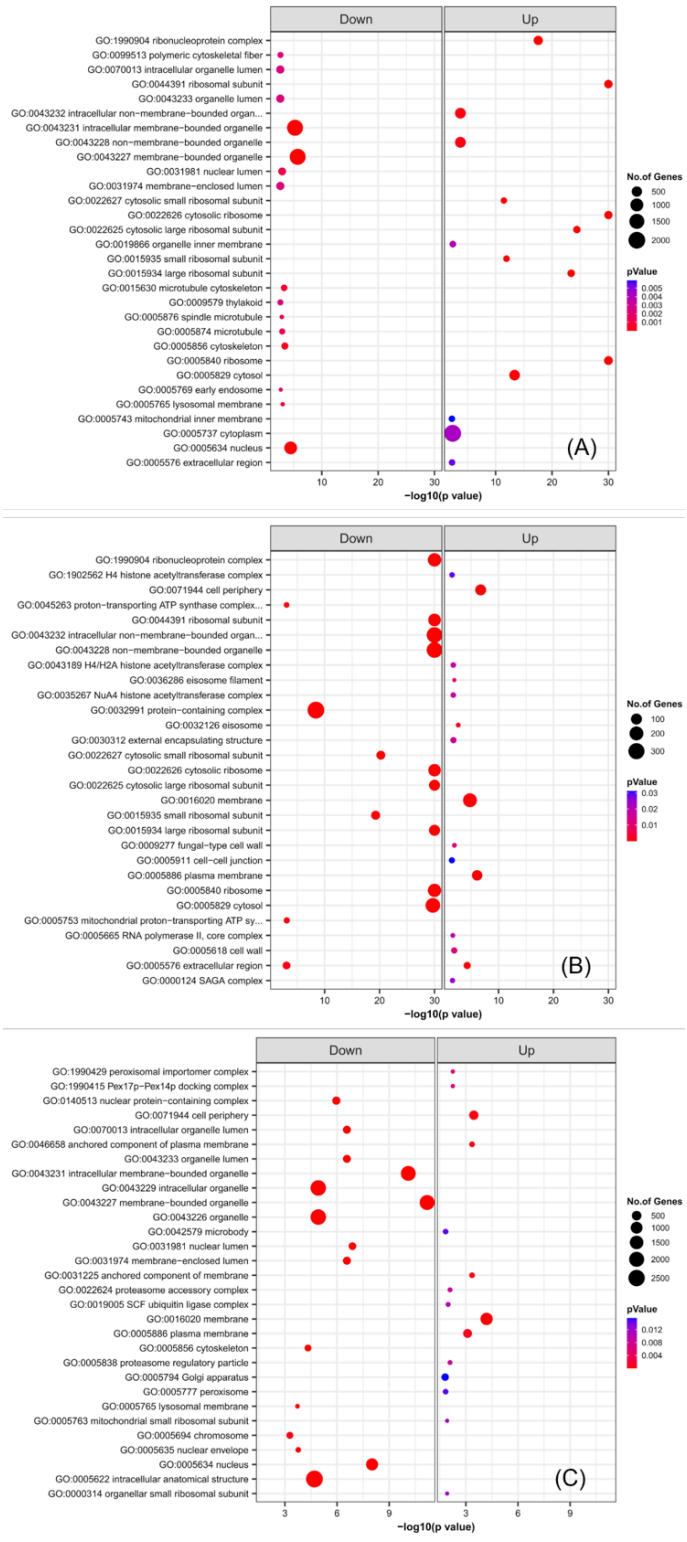

Supp Figure 1: Dot plot of the enriched cellular components (CC) GO terms annotated to the DEUs in **(A)** *Sabal miamiensis* vs *Pseudophoenix sargentii,* **(B)** *Sabal miamiensis* vs *Sabal palmetto,* and **(C)** *Sabal palmetto* vs *Pseudophoenix sargentii*. The size of each dot is proportional to the number of genes associated with the corresponding GO term and color gradience is with respect to the *p*-value.

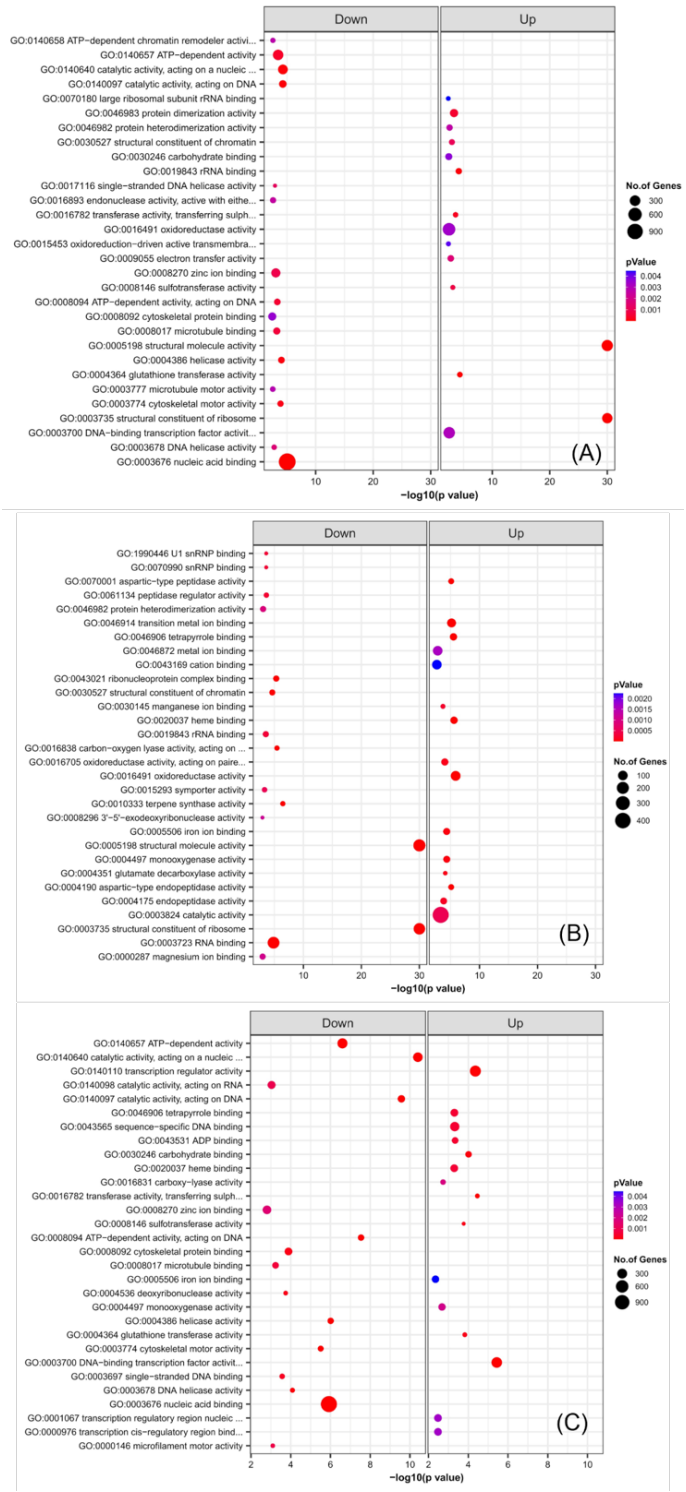

Supp Figure 2: Dot plot of the enriched Molecular Function (MF) GO terms annotated to the DEUs in **(A)** *Sabal miamiensis* vs *Pseudophoenix sargentii,* **(B)** *Sabal miamiensis* vs *Sabal palmetto,* and **(C)** *Sabal palmetto* vs *Pseudophoenix sargentii*. The size of each dot is proportional to the number of genes associated with the corresponding GO term and color gradience is with respect to the *p*-value.